

Supporting Information

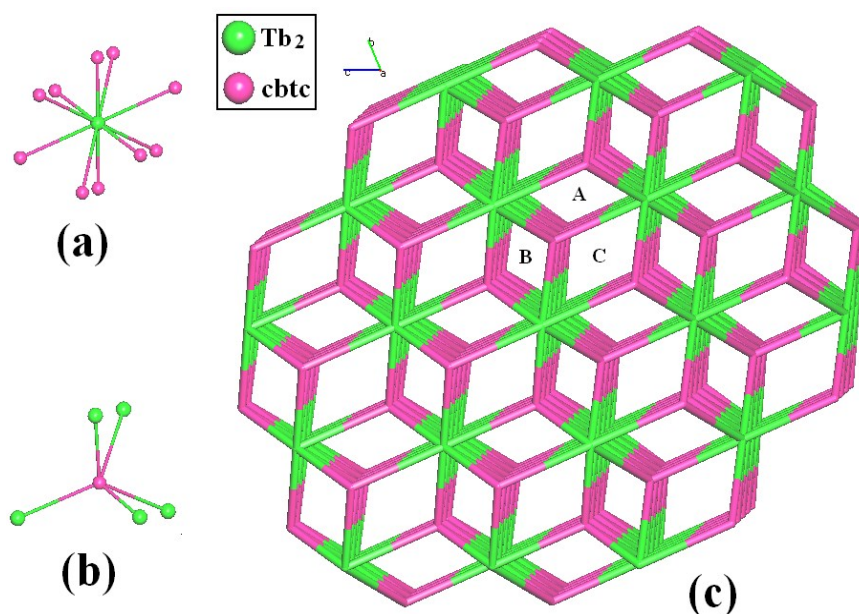


Figure S1 (a) 10-connected Tb₂ core node; (b) 5-connected Hcbtc ligand node; (c) (5,10)-connected 3D topology framework for Tb-Tb

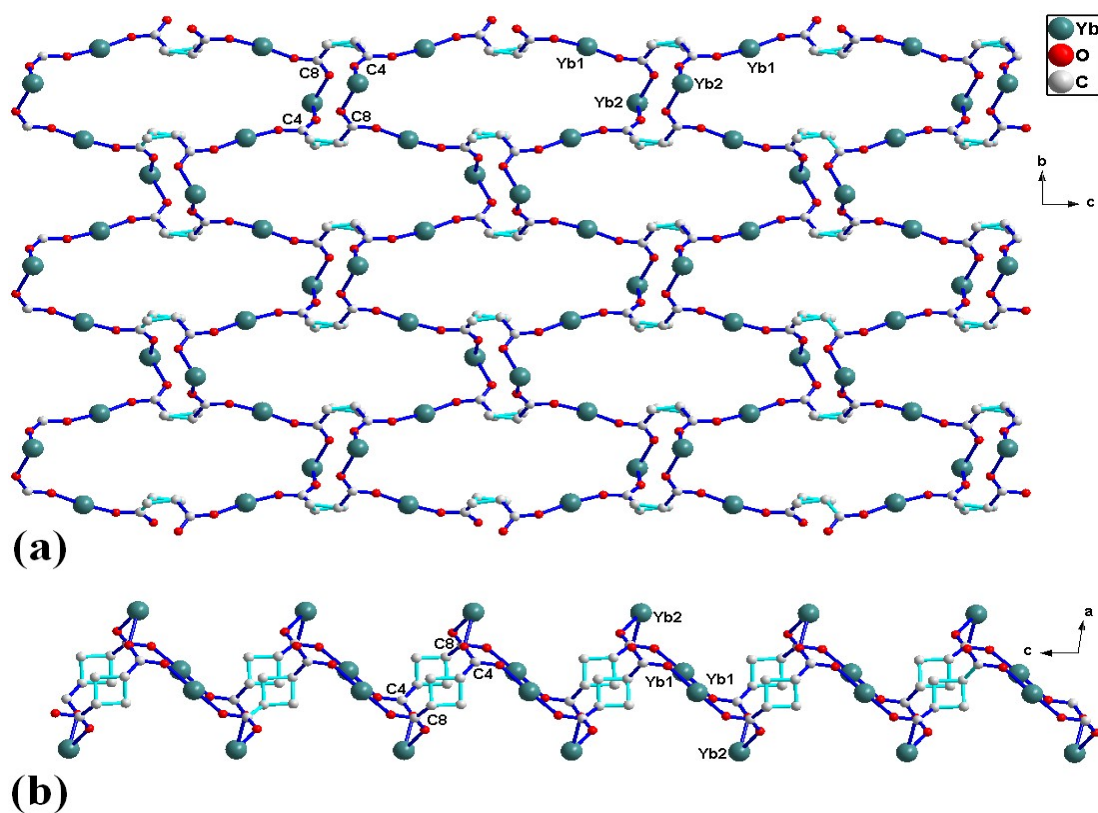


Figure S2 (a) and (b) the 2D layer structures connected by carboxylated groups -C4OO and -C8OO along *a* and *b* axis, respectively.

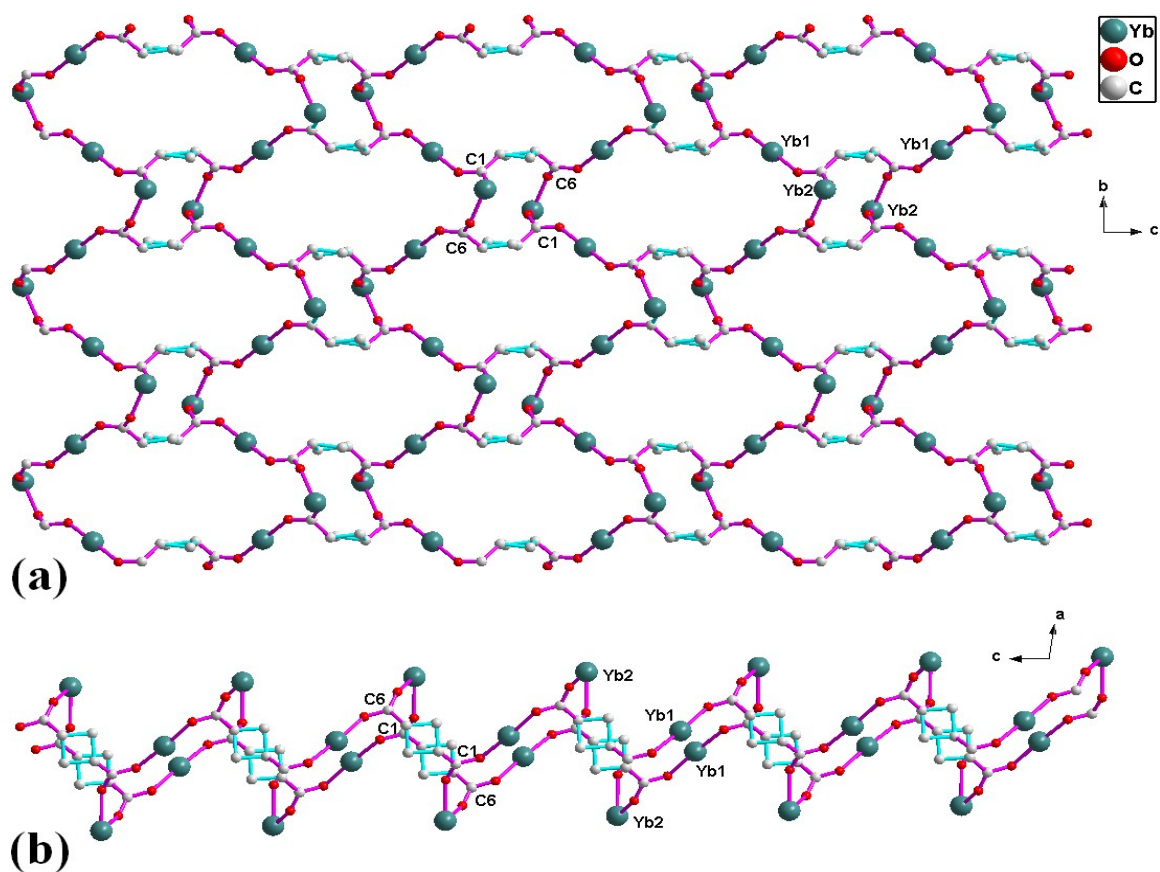


Figure S3 (a) and (b) the 2D layer structure connected by carboxylated groups -C1OO and -C6OO along *a* and *b* axis, respectively.

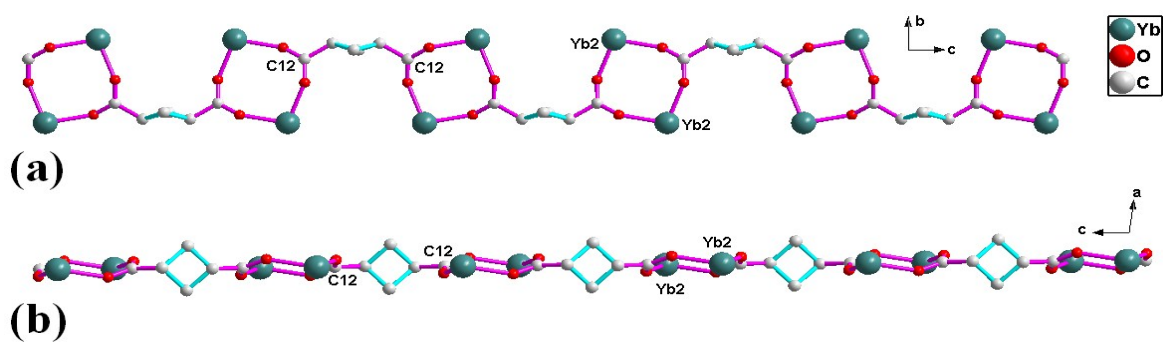


Figure S4 (a) and (b) the 1D chain structure constructed from Yb₂Yb₂ unit and the carboxylate group -C12OO along *a* and *b* axis, respectively.

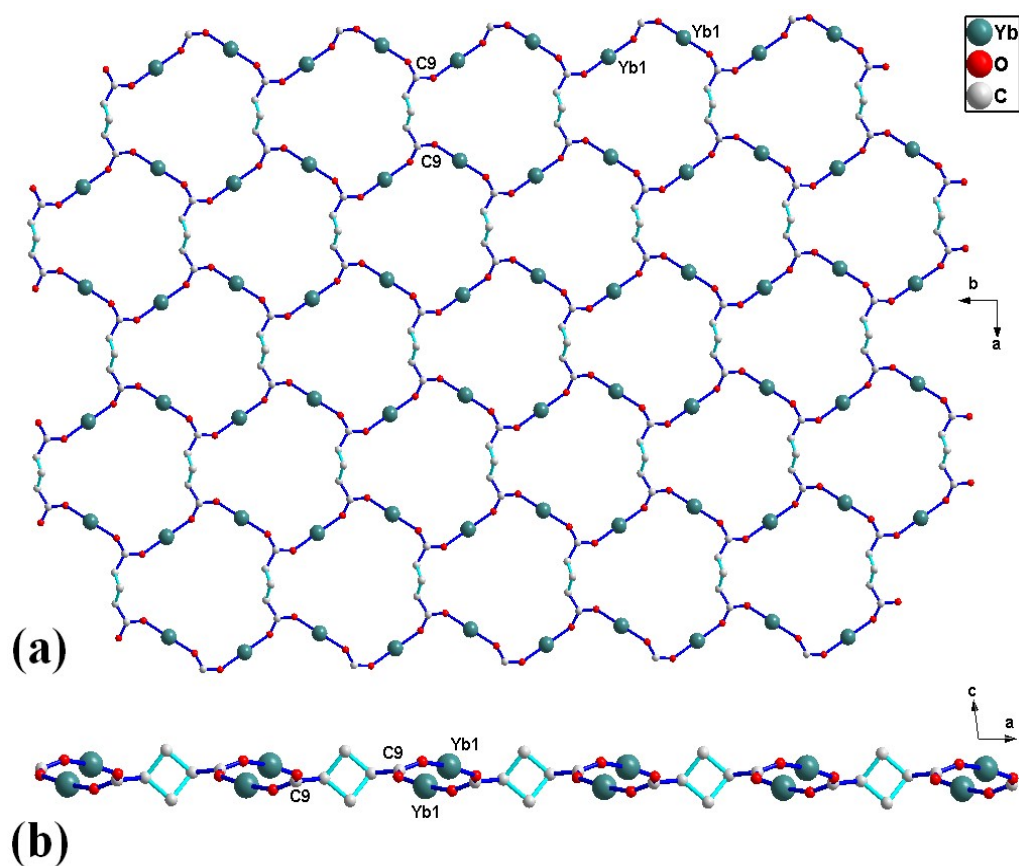


Figure S5 (a) and (b) the 2D layer structure connected by carboxylated group -C9OO and Yb1Yb1 unit along *c* and *b* axis, respectively.

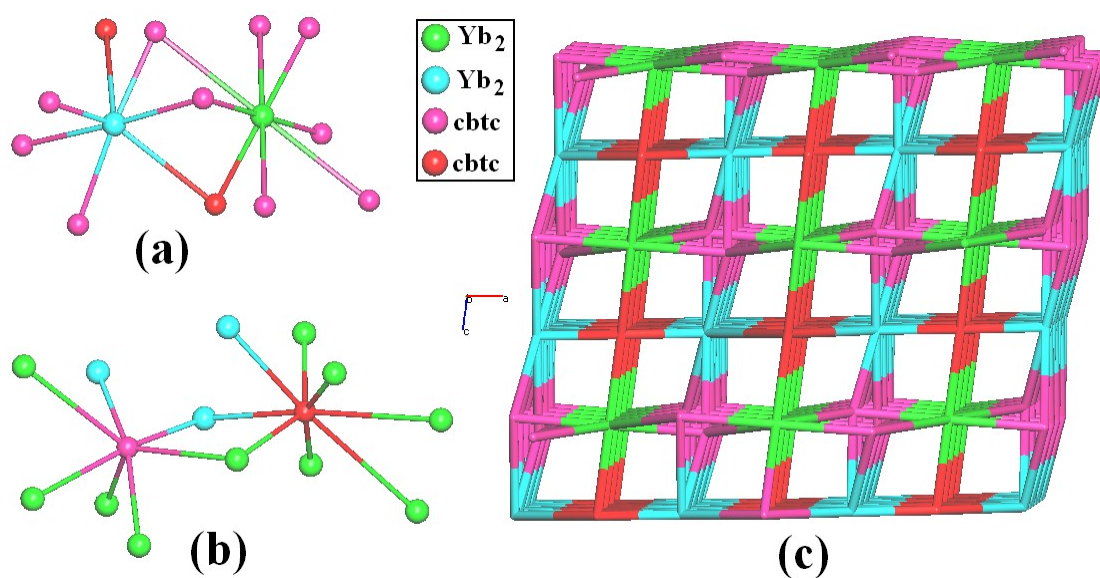


Figure S6 (a) and (b) (7, 8)-connected Yb_2 cluster and cbtc ligand nodes, respectively. (c) (7,7,8,8)-connected 3D topology framework.

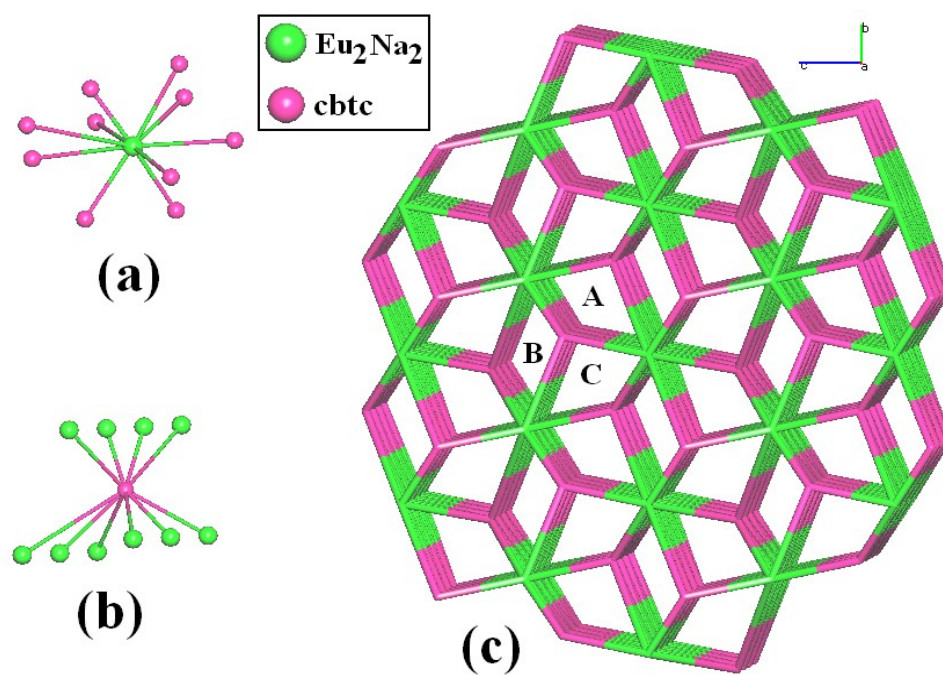


Figure S7 (a) and (b) 10-connected Eu_2Na_2 cluster and cbtc ligand nodes, respectively; (c) (10,10)-connected 3D topology framework.

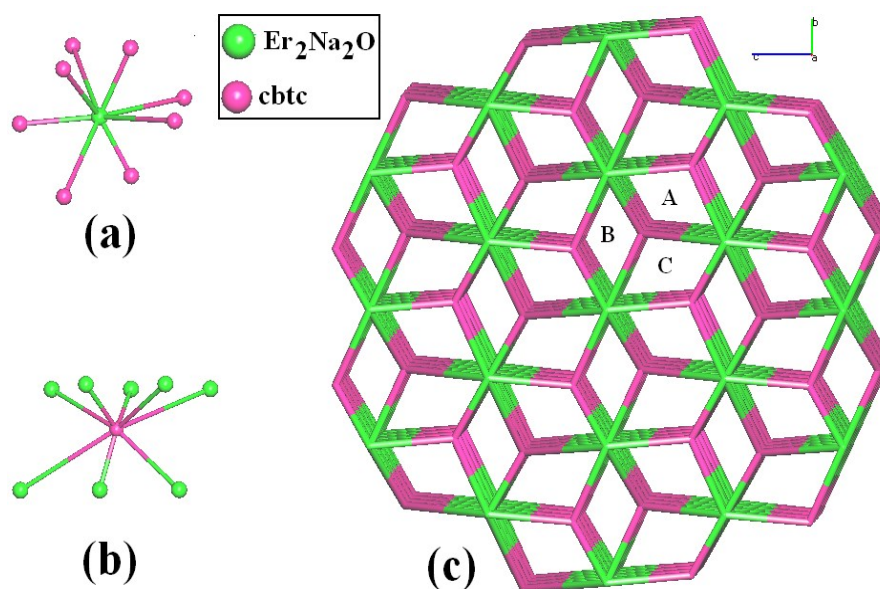


Figure S8 (a) and (b) 8-connected $\text{Er}_2\text{Na}_2\text{O}$ cluster and cbtc ligand nodes, respectively; (c) (8,8)-connected 3D topology framework.

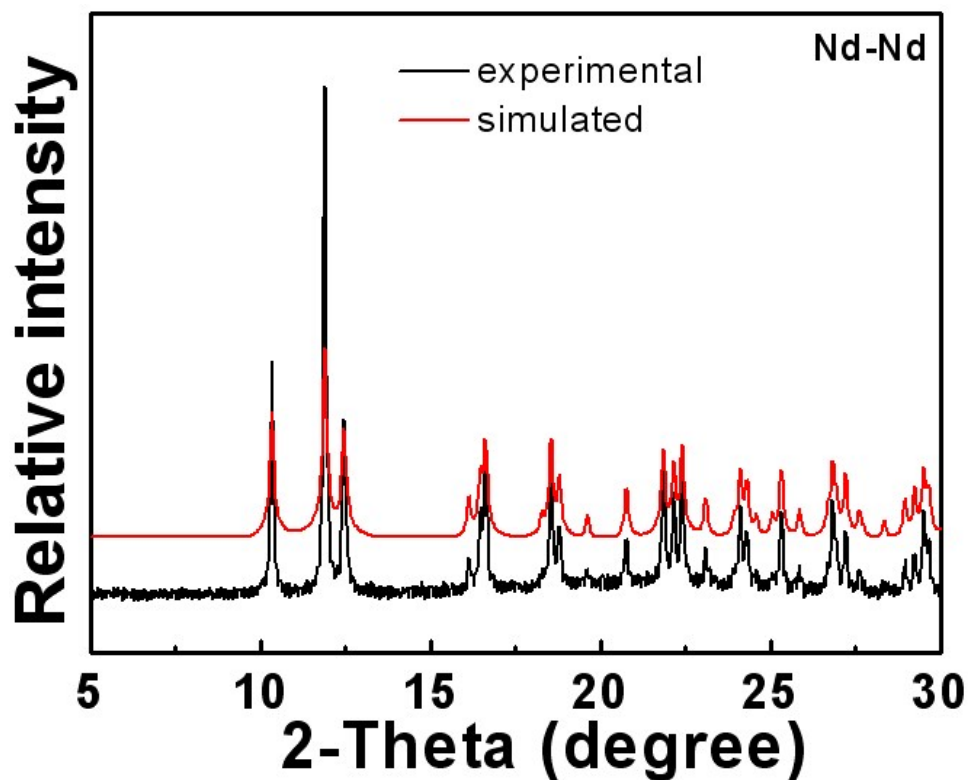


Figure S9 The experimental and simulated PXRD patterns for Nd-Nd. The top is the simulated pattern, and the bottom is the experimental one.

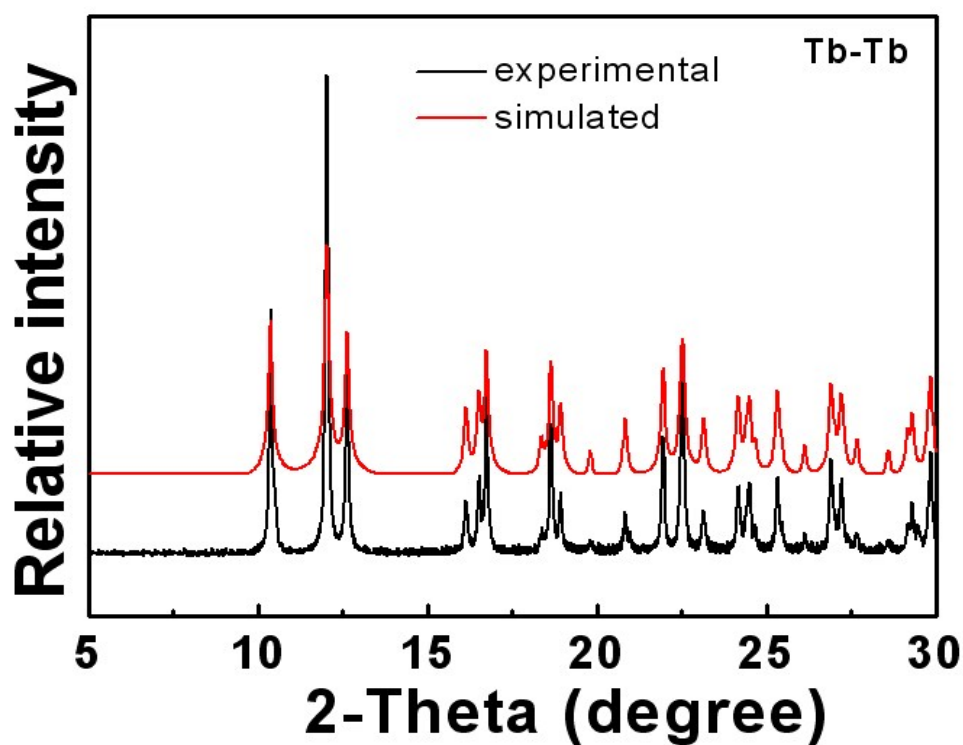


Figure S10 The experimental and simulated PXRD patterns for Tb-Tb. The top is the simulated pattern, and the bottom is the experimental one.

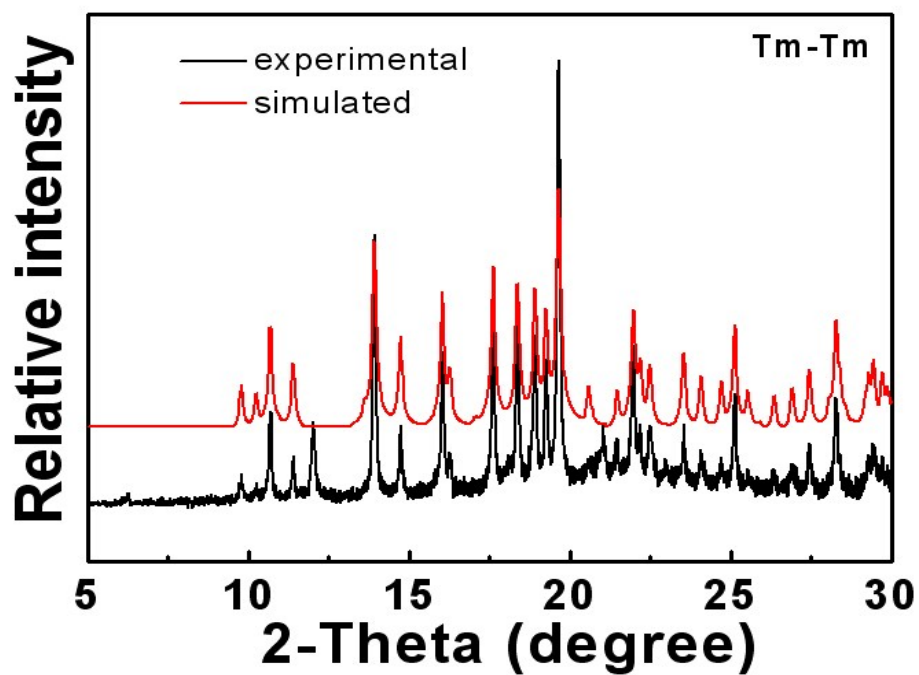


Figure S11 The experimental and simulated PXRD patterns for **Tm-Tm**. The top is the simulated pattern, and the bottom is the experimental one.

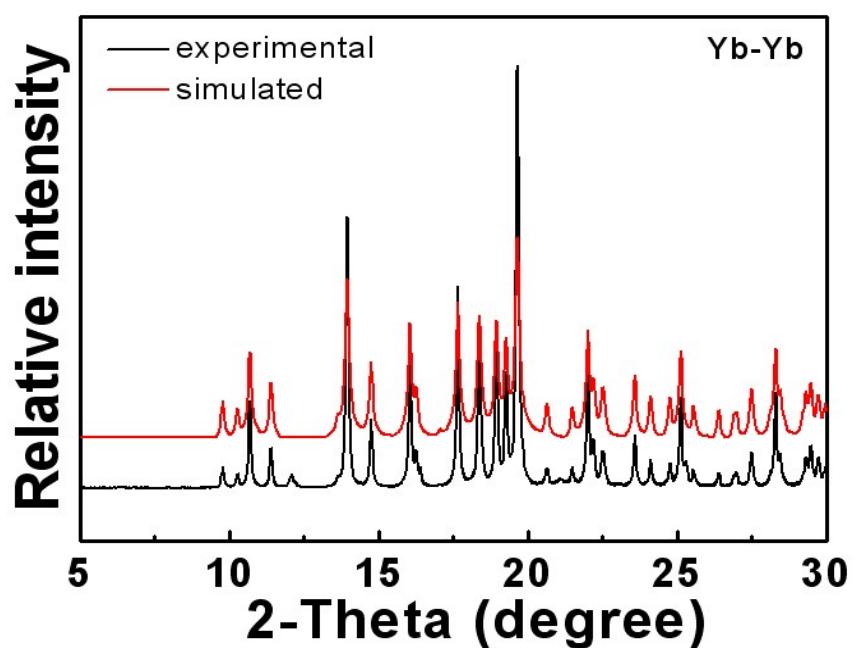


Figure S12 The experimental and simulated PXRD patterns for **Yb-Yb**. The top is the simulated pattern, and the bottom is the experimental one.

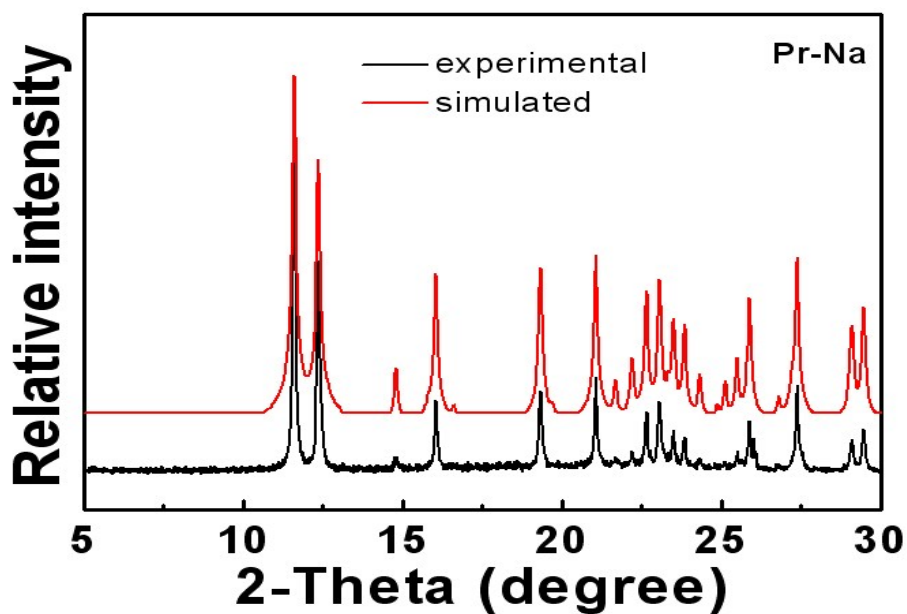


Figure S13 The experimental and simulated PXRD patterns for **Pr-Na**. The top is the simulated pattern, and the bottom is the experimental one.

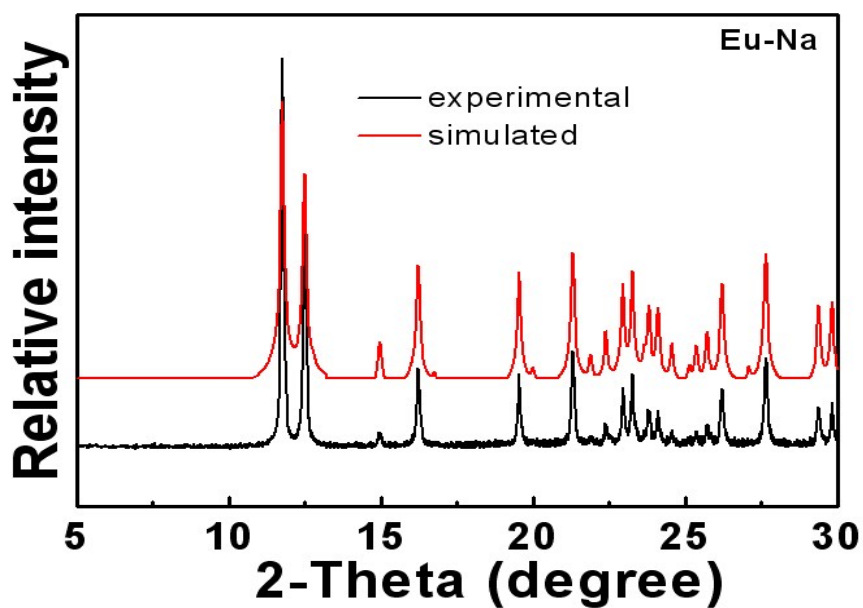


Figure S14 The experimental and simulated PXRD patterns for **Eu-Na**. The top is the simulated pattern, and the bottom is the experimental one.

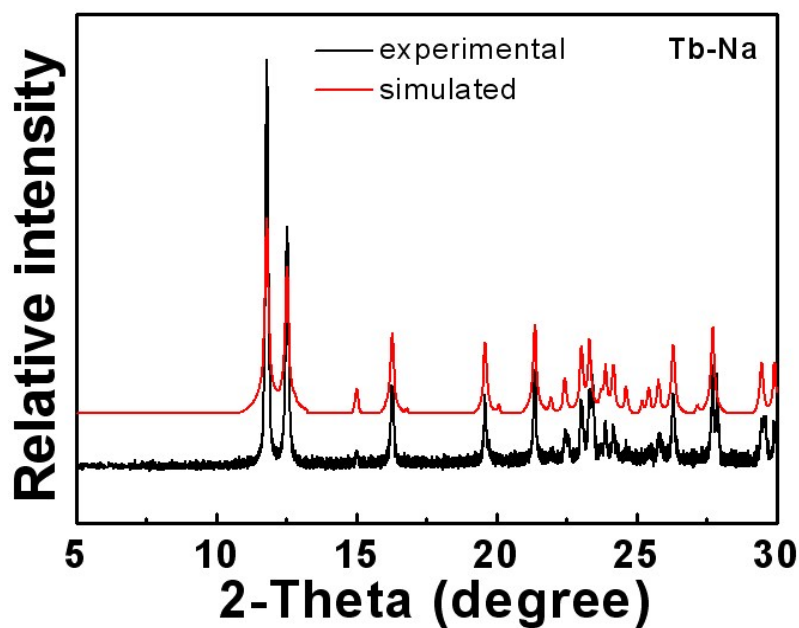


Figure S15 The experimental and simulated PXR D patterns for **Tb-Na**. The top is the simulated pattern, and the bottom is the experimental one.

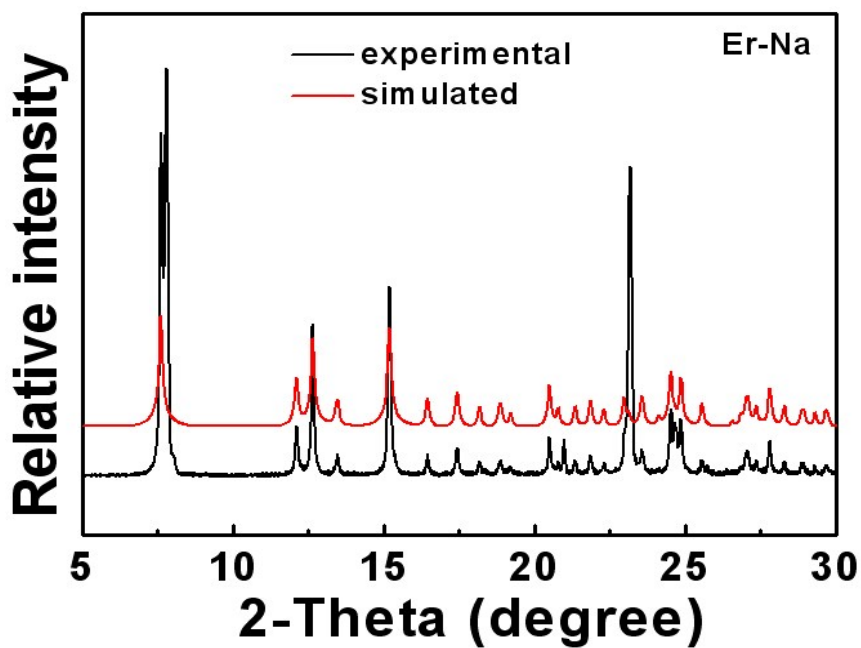


Figure S16 The experimental and simulated PXR D patterns for **Er-Na**. The top is the simulated pattern, and the bottom is the experimental one.

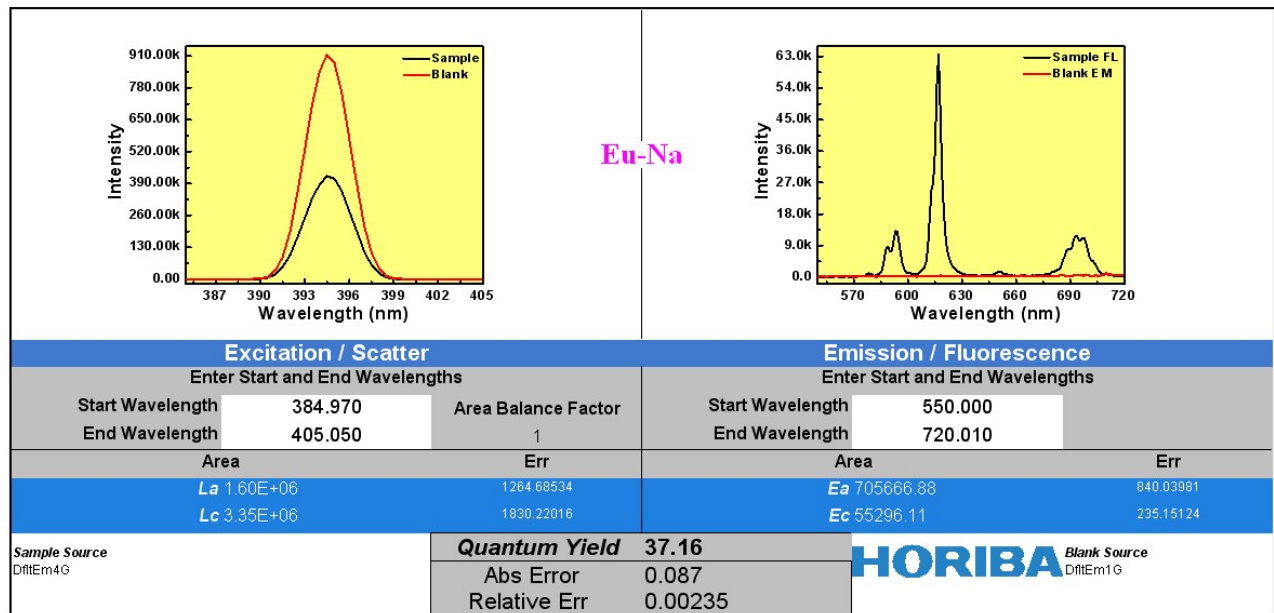
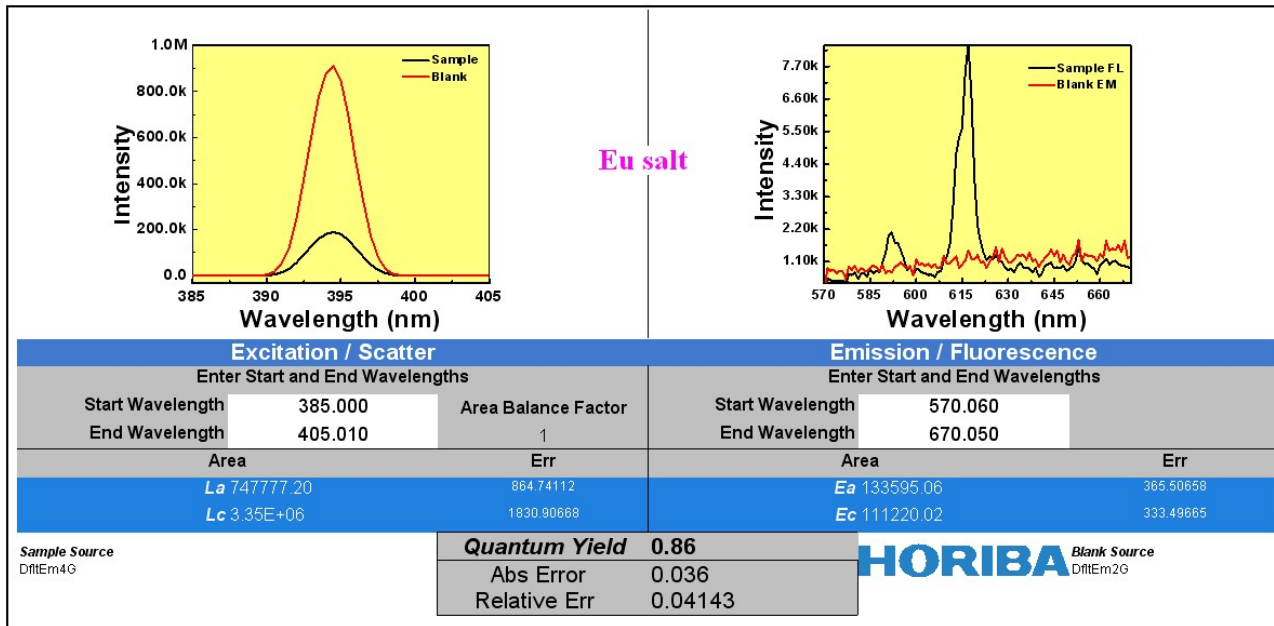


Figure S17 The measurement details of solid state fluorescence quantum yield for **Eu salt** (top) and **Eu-Na** (down)

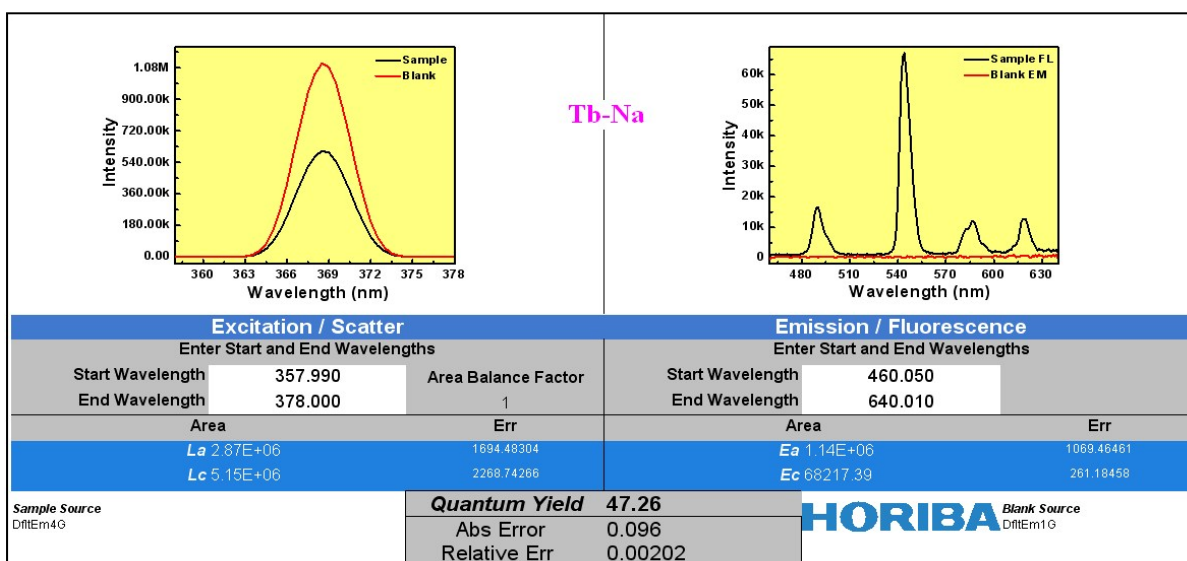
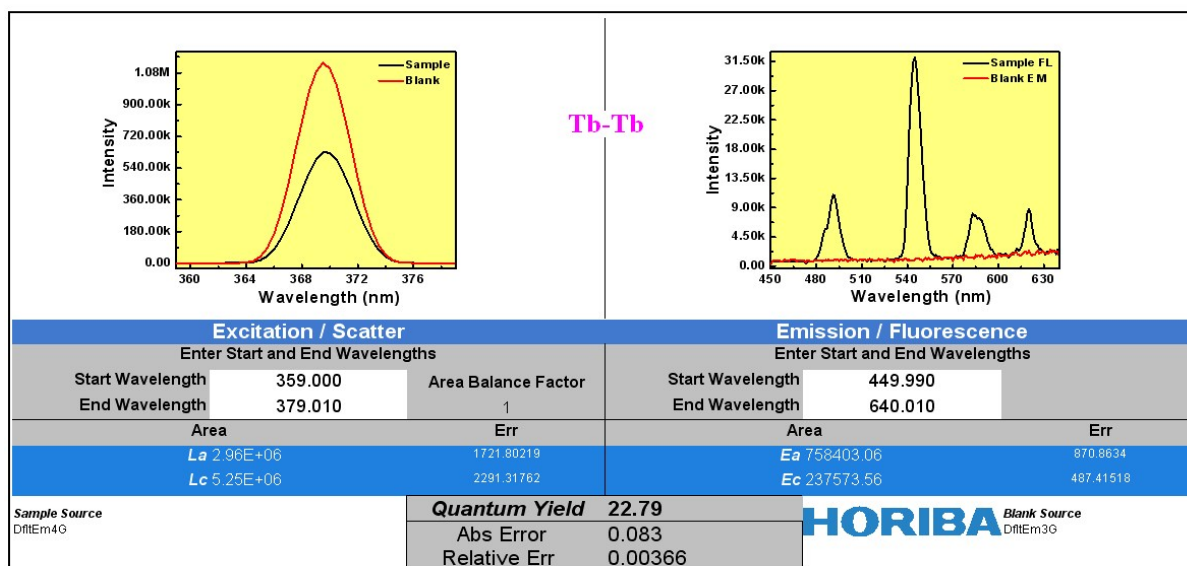
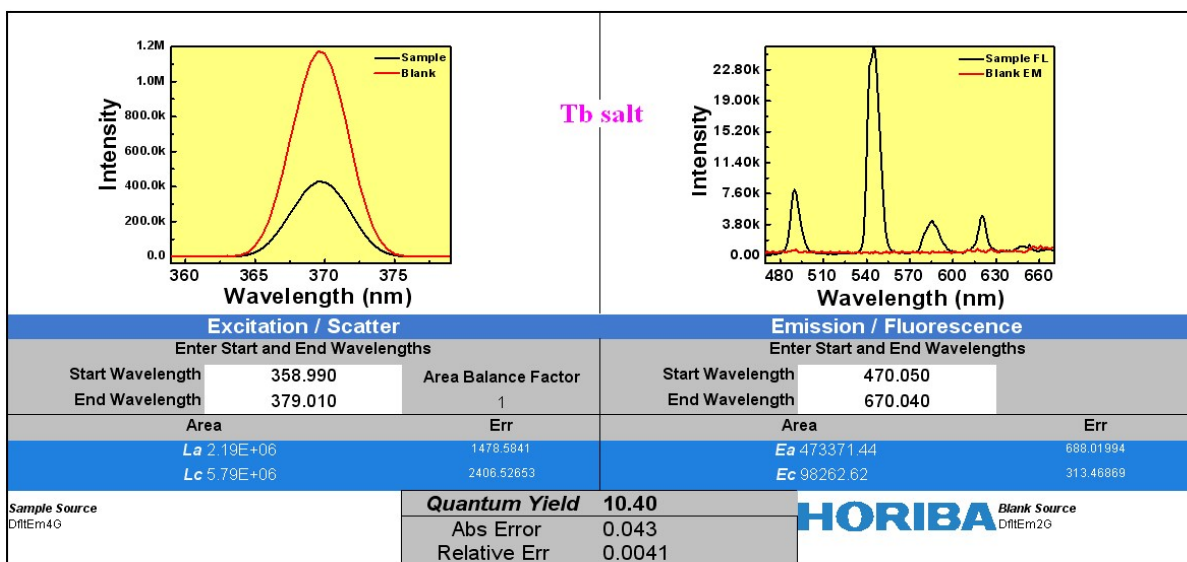


Figure S18 The measurement details of solid state fluorescence quantum yield for **Tb salt** (top) **Tb-Tb** (middle) and **Tb-Na** (down)

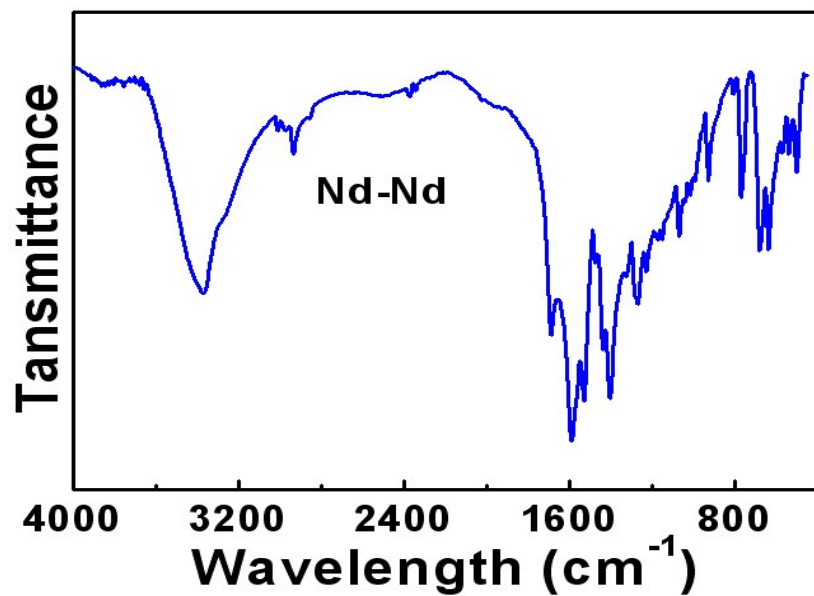


Figure S19 FT-IR spectra for Nd-Nd

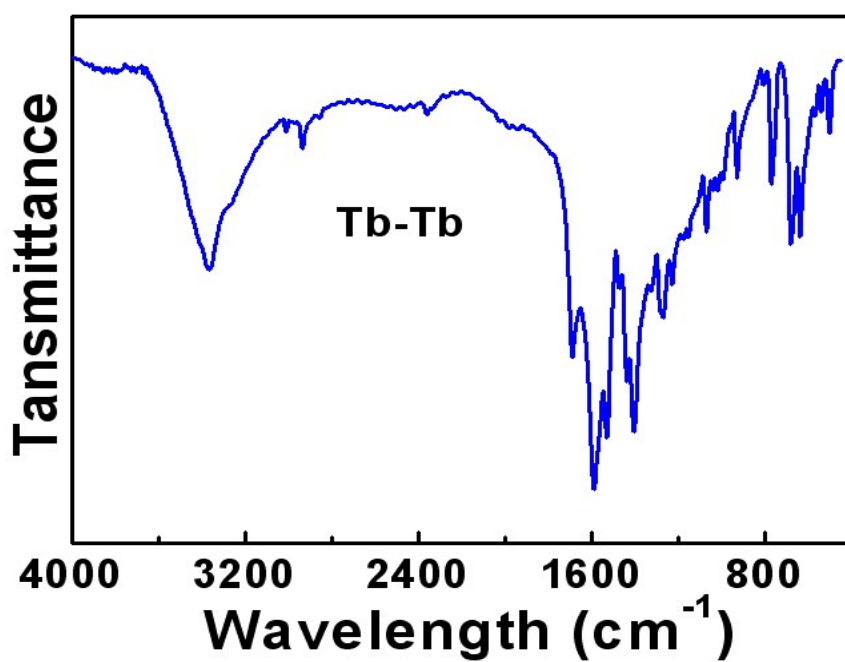


Figure S20 FT-IR spectra for Tb-Tb

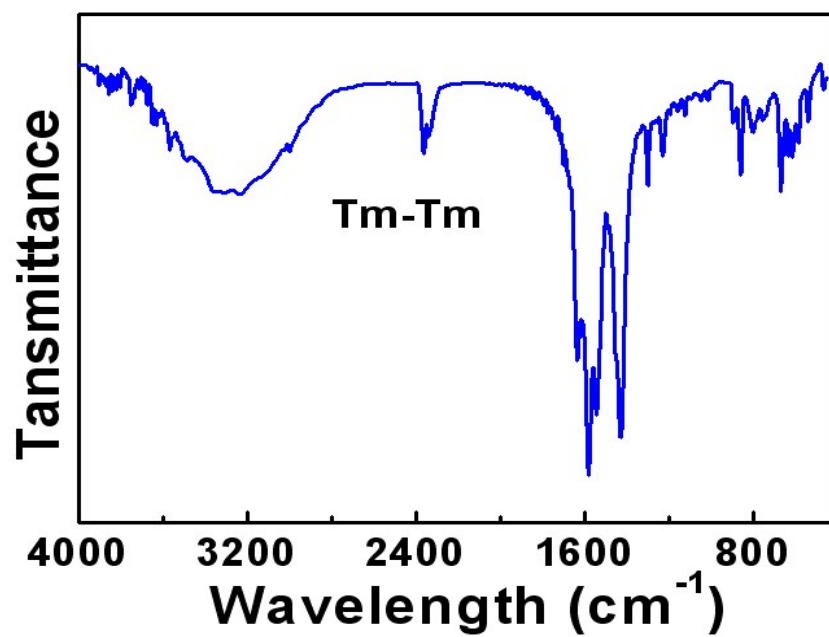


Figure S21 FT-IR spectra for Tm-Tm

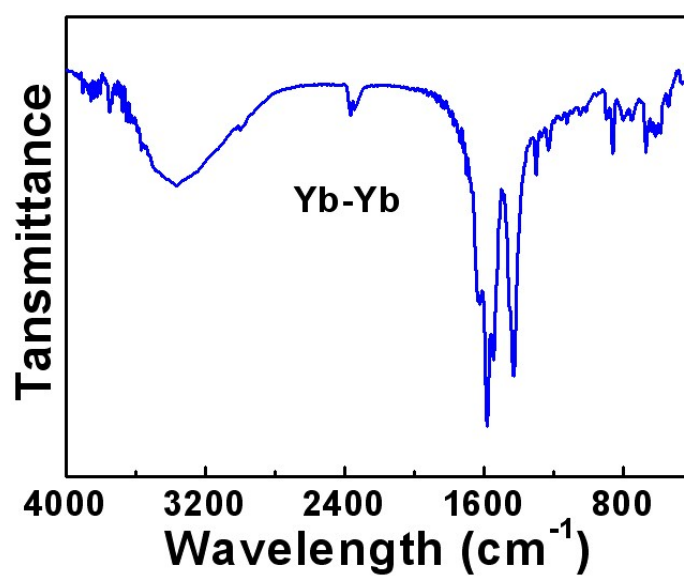


Figure S22 FT-IR spectra for Yb-Yb

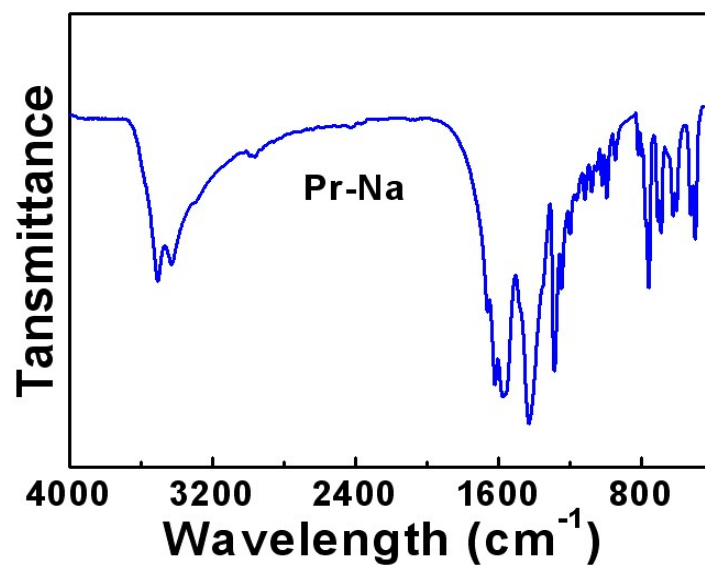


Figure S23 FT-IR spectra for Pr-Na

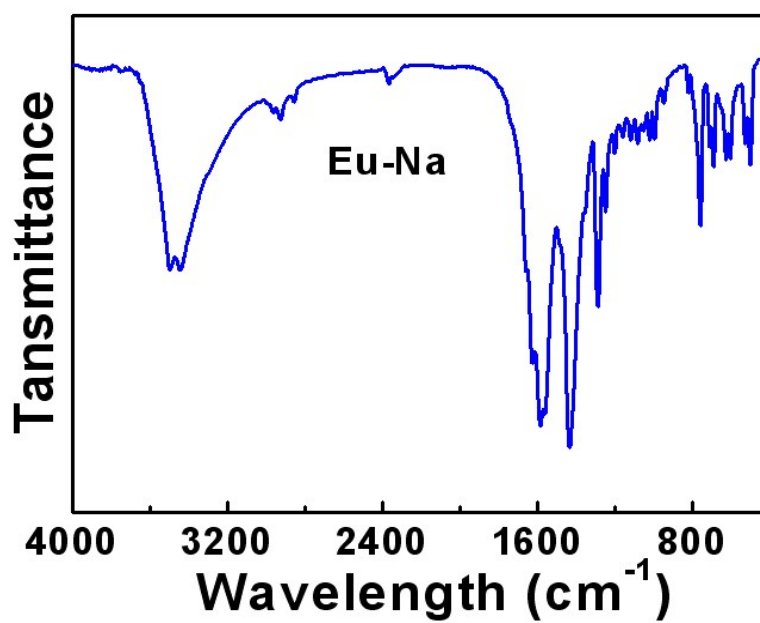


Figure S24 FT-IR spectra for Eu-Na

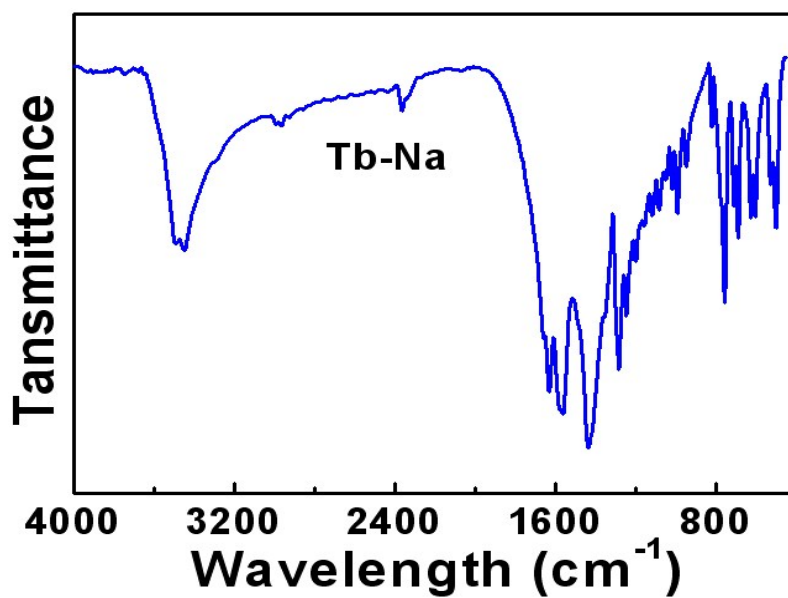


Figure S25 FT-IR spectra for Tb-Na

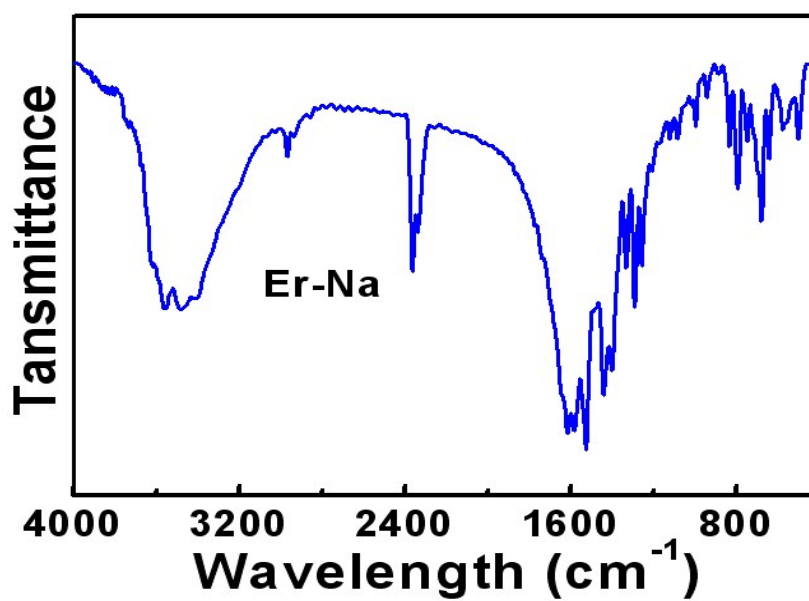


Figure S26 FT-IR spectra for Er-Na